Proceeding of the IEEE
International Conference on Robotics and Biomimetics
Dali, China, December 2019

# Full-Drive Decoupled Bionic Finger: Structure and Experimental Trials*

Liyao Zhu, Wenbiao Wang, Zhicheng Tao, Bangchu Yang, Zhipei Chen, Han Ge and Guanjun Bao*

*College of Mechanical Engineering*
*Zhejiang University of Technology*
*Hangzhou, Zhejiang Province, China*

gjbao@zjut.edu.cn

***Abstract* - This paper presents the design and pilot experiment of a novel full-drive decoupled bionic finger with four degrees of freedom (DOFs). Each joint of the proposed finger can operate independently, without interference from its company. Three pneumatic artificial muscles and a steering engine serve as the drivers for all the four joints, which ensures their independent motions. More specifically, the pneumatic artificial muscles drive the distal interphalangeal (DIP), middle interphalangeal (MIP) and proximal interphalangeal (PIP) joints, who can realize flexion. The steering engine drives the metacarpophalangeal (MP) joint, which performs the adduction and abduction motion. Tendons transfer power from the pneumatic artificial muscles and drive the front three joints with compliance. Different from the traditional tendon drive systems, we proposed a new *N* type tendon drive scheme, which enables the decoupling between the joints with just one single tendon driving single joint. The MP joint is driven separately by the steering engine and has no influence from other joints. With the characteristics of full-drive and decoupling, the bionic finger has less demand for sophisticated mathematical model and control algorithm, and can achieve precise position and orientation through relatively simple controller. Finally, the motion and grasping experiments demonstrated the full-drive and decoupling features, which implies the possibility for future application in dexterous hand development and practice.**

***Index Terms – bionic finger, decoupling, full-drive, pneumatic artificial muscle, dexterous hand***

## I. INTRODUCTION

In the past decades, robots have been continuously deployed in industry, as well as other possible fields. However, the current robot end-effectors in practice, only a simple gripper in most cases, are confined to simple grasping action and cannot operate as that of human being [1]. A humanoid dexterous hand has the characteristics of multiple joints and degrees of freedom (DOFs), which could replace humans to do a mass of jobs and operations. To expend the application area of the end-effector to industrial lines, service robots, aerospace, disaster rescue, and other fields, a large number of humanoid dexterous hands have emerged [2-4].

In terms of driving mode, dexterous hands could be classified into two categories: under-actuated and full-drive. Pisa//IIT softhand2 [5] is a typical under-actuated dexterous hand with 19 joints, five of whom are simple revolute joints, which realize the adduction/abduction of the hand movement. The remaining 14 joints are rolling contact nodes that could bend adaptively. All joints are driven by the antagonism of two motors. When the motor moves in the same direction, the tendons short themselves to close the soft hand. Conversely, the hand will stretch. However, this hand could only realize a few specific gestures and grasp target objects with a few certain poses. While operating, the softhand2 is unable to change its posture to adapt to various tasks. In some special human operations such as pinch, which only needs the fingertip of the thumb and index finger, other fingers will flexion passively, which would have an indestructible adverse effect on these tasks. SSSA-MyHand [6] is another representative under-actuated dexterous hand with five fingers, each of whom has two joints. It has three motors, among which one motor drives the flexion of the thumb. One other motor drives the adduction/abduction of the thumb and flexion of the index finger, and the third motor drives all joints of the remaining three fingers. A four-link mechanism couples the two joints of the four fingers, and the Geneva mechanism couples the adduction/abduction of the thumb and flexion of the index finger. Consequently, SSSA-MyHand could only achieve some simple grasping movements, unable to achieve finger movement with different joint angles. Therefore, when grasping objects of different sizes and shapes, the hand may not be able to grasp the objects or even damage the objects, due to the coupled movement of the three fingers. Other under-actuated hands [7-10] in current studies all have the same limitations, which therefore limits their application to massive areas where sophisticated or agile manipulation exists.

Full-drive dexterous hands are developed to fill up the deficiency of their under-actuated counterparts. For example, 5-fingered shadow dexterous hand [11] employs 40 pneumatic muscles to drive its 20 independent joints and 4 coupled joints. The thumb has 5 DOFs and the other four fingers have the same structure of 4 joints and 3 DOFs with the end joint coupled to the middle joint. Furthermore, the Shadow dexterous hand has one DOF in the palm and two DOFs in the wrist. The hand could achieve various kinds of precision grasping and manipulation. However, the Shadow dexterous hand achieves joint movement and reset by two coupled artificial pneumatic muscles, which results in the quite big number of actuators and swollen arm. Although compared with

* This work is supported by NSFC No. 51775499, 51605434 and Fundamental Research Funds for the Provincial Universities of Zhejiang No. RF-C2019004.



978-1-7281-6321-5/19//$31.00 ©2019 IEEE

the $N$+1 type, it eliminates the decoupling process and enables independent joints, dozens of actuators will still challenge the control algorithm. Additionally, Robonaut 2 Hand [12], UTAH/M.I.T. dexterous hand [13] and UBH hand [14] are all full-drive dexterous hands, which were designed in $N$+1 type or 2$N$ type of tendon drive system. Inevitably, they all have some problems of actuator cluster and controlling strategy. Besides, there are also motor-drive dexterous hands, such as DLR/HIT hand [15, 16]. Such dexterous hands have the problems of excessive weight of the finger and high cost, due to built-in actuators and sensors.

If the easy control of the under-actuated dexterous hand and the agile performance of the full-drive dexterous hand could be combined into one dexterous hand, the application of the dexterous hand and the adaptability to the environment will be significantly increased. Based on this concept, we designed the bionic finger in this paper. The bionic finger has four joints, three of which use torsion springs to reset the joints and pneumatic artificial muscles as actuators. Moreover, we propose a new $N$ type tendon drive system, in which each actuator individually controls its corresponding joint. At the same time, we optimized the arrangement of the tendon route, to make sure that the driving tendon of the distal phalanx, through the rotational axis of the proximal phalanx. By this method, the torque of the distal phalanx driving tendon to the proximal phalanx is zero. The steering engine independently controls the fourth joint. Therefore, there is no coupling among the joints, which reduces the complexity of the control algorithm.

The specific arrangement of this paper is as follows. In section II, the distribution of DOF of the bionic finger, the principle of full drive and decoupling are introduced. Section III introduces the arrangement of the sensor, the choice of the actuator, and the components of the experimental platform. Finally, we performed the bending, grasping, and interactive experiments for the prototype. The experiments proved the high performance of the proposed full-drive decoupled bionic finger (FDB finger).

## II. Structure Design of Bionic Finger

### A. Mechanism scheme

The finger of the under-actuated dexterous hand can only achieve some specific bending posture during the grasping process, and cannot independently control each joint of the finger. Therefore, the movement of the finger joint will be limited by the shape of its target object during the grasping action of the whole hand. Moreover, due to the fixing position of the thumb of the under-actuated dexterous hand relative to the four fingers, the hand can only perform several different postures and grasp objects with regular shapes. Trying to avoid the disadvantage, we designed a full-drive decoupled bionic finger. Each joint of the bionic finger can be driven independently. In the process of grasping, the motion angle of each joint can be planned to realize the pre-grab action. Moreover, we added an adduction/abduction joint to the end of the finger so that the bionic finger could realize a swinging motion. Therefore, the multi-finger structure can realize different gestures and grasping target objects of different shapes. According to the anatomical structure, the index finger, the middle finger, the ring finger and the little finger of the human hand have three joints, two of which can be flexion, and the other can be adduction/abduction and flexion. The thumb has three joints, one as flexion and the other two as adduction/abduction and flexion. In order to modularize the structure, we designed a bionic finger with four DOFs according to the mechanism of thumb and the other four fingers. At the same time, in order to simplify the design, the joint that can perform adduction/abduction and flexion was realized by two independent joints, which have mutually perpendicular rotating axes. Finally, the bionic finger was designed and prototyped, which has three flexion joints and one adduction/abduction joint, as shown in Fig. 1.

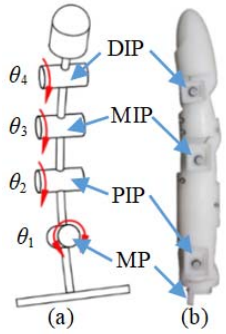


Fig. 1 Full-drive decoupled bionic finger (a) schematic diagram (b) prototype

In Fig. 1, DIP is the distal interphalangeal joint, MIP is the middle interphalangeal joint, PIP is the proximal interphalangeal joint, and MP is the metacarpophalangeal joint. The angles $\theta_2$, $\theta_3$, and $\theta_4$ represent the flexion joints of the bionic finger, ranging from 0° to 90°. The angle $\theta_1$ is the adduction/abduction joint of the bionic finger, within the range of [-30°, 30°].

### B. Full-drive design

There are two driving types of the finger: the built-in actuator and the external actuator. In general, motor is suitable for the built-in actuator. However, motor always needs gear reducer. When the actuator and reducer are embedded inside the finger, there arise the problem of overweight for the finger, which will sharply lower the load/weight ratio. In our work, the actuators that drive the three flexion joints were externally fixed to the finger. Since the adduction/abduction joint locates near the base, it is advantageous to design the built-in actuator. Thus, we can omit the transmission mechanism, without increasing the weight of the finger. Therefore, we used the steering engine as the actuator of the adduction/abduction joint, which was directly mounted on the end of the bionic finger. Also, a groove matching the steering engine was designed, and the rotating shaft was mounted on the opposite side of the engine output shaft. The above mechanical structure ensures the stability of the finger installation and the power output of the steering engine, as shown in Fig. 2. The direct installation of the steering engine simplifies the transmission and makes the bionic finger more compact.

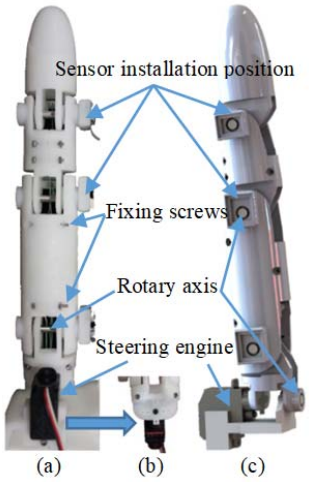


Fig. 2 Bionic finger (a) prototype (b) installation of steering engine (c) three-dimensional model

Since the actuators of the three flexion joints of the single bionic finger were external, the transmission mechanism was required to transmit the actuator's force to the joint. The traditional gear transmission will make the mechanism too complicated and overweight. Moreover, the belt transmission method requires multiple belt pulleys, which will cause the entire finger to be too large and complicated in structure and size, due to the pre-tightening mechanism. Whereas the tendon drive system only needs a single cable to transmit the force to the joint. Compared to the gear and belt transmission, it has a simple structure, and the installation of the tendon is easier. Therefore, we chose the tendon drive system as the transmission of the finger.

Generally, there are three categories of tendon drive system: *N* type, *N*+1 type, and 2*N* type. As shown in Fig. 3 (a), *N* type is suitable for the rotary motor drive. The two tendons drive the joint through the rotation of the motor. There is a problem of tendon relaxation, since the two tendons are affixed to one motor. Therefore, it is necessary to pre-tension the tendon. In addition, the single bionic finger with three joints will need six tendons. Each tendon needs to be pre-tensioned and totally six pre-tightening mechanisms are required. Excessive pre-tightening mechanisms will cause the entire finger to be too complex. As shown in Fig. 3(b), the *N*+1 type drives the movements of *N* joint by *N*+1 tendons. *N*+1 type will cause coupling movement between the joints. When only single joint motion is expected, multiple tendons are required to decouple. Also, the same tendon may be the driving tendon for one joint and the reset tendon for another joint. When we need to drive multiple joints at the same time, it is necessary to constantly change the movement state of the multiple tendons, which leads to the complexity of the control algorithm. Fig. 3(c) demonstrates the 2*N* type, which uses two tendons to drive the motion of one joint. Obviously, the number of actuators is twice of the degrees of freedom. Excessive actuators increase the complexity of mechanical structure and difficulty of the control algorithm. In this work, we designed a new *N* type tendon drive system. Single tendon was used to drive individual joint, and the actuator was used to pre-tighten the tendon. The joint was reset by a torsion spring, as shown in Fig. 3(d). When tendon drives the joint to move, the torsion spring stores the energy. When the actuator releases the tendon, the finger can be passively reset. Compared to the *N* type, we reduced the number of tendons and omitted the pre-tightening mechanism. Compared to the *N*+1 type, we greatly simplified the control algorithm and reduced a certain number of tendons. Compared to the 2*N* type, we reduced the number of actuators, tendons, and the overall size of the bionic finger.

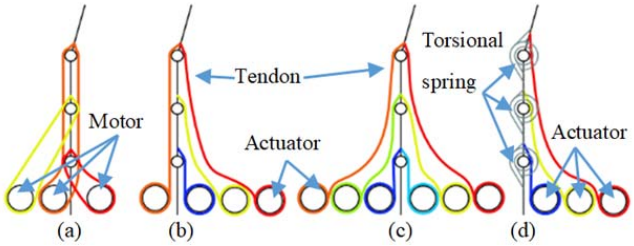


Fig. 3 Types of tendon drive system (a) *N* type (b) *N*+1 type (c) 2*N* type (d) new *N* type

### C. *Decoupling analysis*

Since the actuator is externally mounted on the finger, the tendon needs to be fixed to the actuator through all the joints. As the tendons will exert extra force on the joint when the tendon passes through during the transmission of the force, a coupling phenomenon occurs between the joints of the finger. This phenomenon disables the independent control of the single joint by single tendon. In general, the fingers driven by the tendons have the phenomenon of joint coupling. Therefore, multiple actuators are required to cooperate to achieve decoupling, which leads to an overly complicated control algorithm. In order to solve the coupling phenomenon between the joints, the tendon drive system needs a reasonable tendon route to eliminate the coupling phenomenon. In this paper, we designed a new tendon route, through which each tendon can independently drive single joint without interfering the movement of other joints. Fig. 4 shows the principle of new tendon route, where $A_1$ is the driving tendon of PIP joint, $A_2$ is the driving tendon of DIP joint, and $A_3$ is the driving tendon of MIP joint. The tendon that drives the DIP joint passes through the rotation axis of MIP, PIP, MP and the tendon that drives the MIP joint passes through the rotation axis of PIP, MP and the tendon that drives the PIP joint passes through the rotation axis of the MP. We optimized the tendon route to achieve decoupling between the joints. Through this special tendon route, it can use one tendon to drive the joint moving without causing the movement of other joints. The steering engine directly applies the output force to the finger and does not cause the coupling phenomenon.

### D. *Arrangement of Sensors*

In order to control the joint rotation of the bionic finger accurately, a fundamental closed-loop was designed with the actual angle feedback and the desired reference. Since the adduction/abduction joint adopted a steering engine that can perform an accurate position control independently by an internal closed-loop, only angles of the other three flexion joints need to be sampled with sensors.

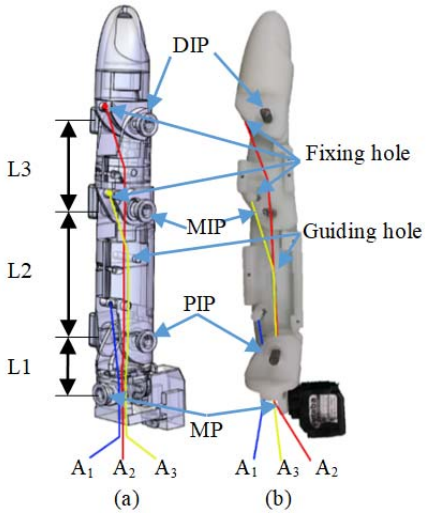


Fig. 4 Tendon route (a) three-dimensional model (b) prototype

We chose the Hall sensor as angle sensor. Compared with the potentiometer, the Hall sensor has a higher detection accuracy. What's more, it will not cause any additional impact on joint motion in the advantage of non-contact. As shown in Fig. 5, we installed the magnetic steel on the outermost side of the rotating shaft through their magnetic force since the material of the rotating shaft is steel. Hence, the installation structure of the magnetic steel can be omitted. The material of the bionic finger is resin, and the bushing used for matching the rotating shaft is made of polyacetal. So, there is no interference with the adsorption of the magnetic steel and the rotating shaft, ensuring the accuracy of the rotation angle. We set up the installation position of the Hall sensor on the outside of the finger and transmitted the angle information to the computer through flexible flat cable.

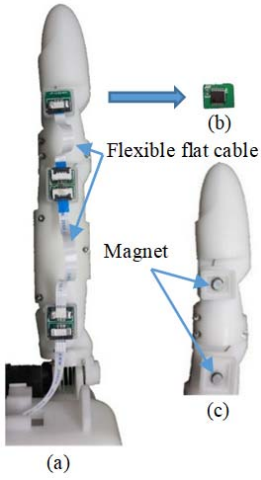


Fig. 5 Arrangement of sensors (a) prototype (b) Hall sensor (c) arrangement of magnetic steel

### E. *Selection of Actuator*

Traditional actuators are generally DC motors, stepper motors, etc. These actuators have inferior performance of human-computer interaction. Therefore, we chose pneumatic artificial muscles as the actuators for the three flexion joints of the bionic finger, as shown in Fig. 6. Pneumatic artificial muscle is an emerging actuator. It is mainly composed of silica gel, which gives it the compliance. It can achieve compliant grasping under the premise of providing sufficient gripping force for bionic fingers, with the similar mechanical characteristics of biological muscle.

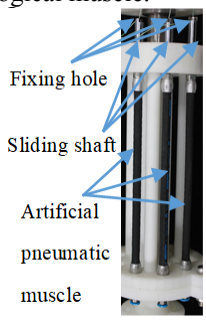


Fig. 6 Pneumatic artificial muscle

## III. Experiment of Full-drive Decoupled Bionic Finger

### A. *Kinematics*

According to the structure of the finger, the DH parameters of FDB finger can be obtained, as shown in the following table, where *i* represents each revolute joint.

TABLE I
DH Parameters

| *i* | $\alpha_{i-1}$ | $a_{i-1}$ | $d_i$ | $\theta_i$ |
|---|---|---|---|---|
| 1 | 0 | 0 | 0 | $\theta_1$ |
| 2 | 90° | L1 | 0 | $\theta_2$ |
| 3 | 0 | L2 | 0 | $\theta_3$ |
| 4 | 0 | L3 | 0 | $\theta_4$ |

According to the DH parameters, the kinematic equation of the FDB finger can be obtained.

$$ {}^{0}_{4}T = \begin{bmatrix} R & P \\ 0^{\mathrm{T}} & 1 \end{bmatrix} \tag{1} $$

where $R$ is the rotation matrix of coordinate system 4 with respect to coordinate system 0, $P$ is the translation vector of coordinate system 4 with respect to coordinate system 0, and $0^{\mathrm{T}}$ is a three-element row vector. In R $\beta=\theta_2+\theta_3+\theta_4$, we can get the result as following:

$$ R = \begin{bmatrix} \cos(\beta)\cos\theta_1 & -\sin(\beta)\cos\theta_1 & \sin\theta_1 \\ \cos(\beta)\sin\theta_1 & -\sin(\beta)\sin\theta_1 & -\cos\theta_1 \\ \sin(\beta) & \cos(\beta) & 0 \end{bmatrix} \tag{2} $$

$$ P = \begin{bmatrix} \cos\theta_1(\mathrm{L1}+\mathrm{L3}\cos(\theta_2+\theta_3)+\mathrm{L2}\cos\theta_2) \\ \sin\theta_1(\mathrm{L1}+\mathrm{L3}\cos(\theta_2+\theta_3)+\mathrm{L2}\cos\theta_2) \\ \mathrm{L3}\sin(\theta_2+\theta_3)+\mathrm{L2}\sin\theta_2 \end{bmatrix} \tag{3} $$

### B. *Experimental Platform*

The experimental platform mainly consists of two sections. One is the control of pneumatic artificial muscles and steering engine and the other is the acquisition of the joint angle.

As shown in Fig. 7, we employed Hall sensor (AS5047P) as angle sensor, SMC's ITV1050-312L as the proportional valve, and equipped with power supply, DC-DC converter, and air pump. For the three flexion joints, the PC controller issues the desired angle. The lower computer obtains the feedback

from the angle sensor and forms a closed loop to achieve accurate position control. For the adduction/abduction joint, the lower computer gets the desired angle from the PC computer and then directly transmits the PWM wave to the steering engine, forming a small closed loop in the steering engine to achieve accurate position control. The PC, STM32, DAC, and proportional valve are mainly used for the control of pneumatic artificial muscles, which can regulate air pressure output accurately. The angle sensor and STM32 realize the information acquisition of joint angle position and steering engine control.

### C. *Experiment*

In order to verify the decoupling of the joints of bionic finger, we performed bending experiment of the finger joints. By comparing Fig. 8(b), (c), (d) and (e), it can be known that when the angle of MP is determined, changing the angles of PIP, MIP, and DIP will not affect the angle of MP. When the angle of PIP is determined, changing the angles of MIP and DIP will not affect the angle of PIP. Also, when the angle of MIP is determined, changing the angle of DIP will not affect the angle of MIP. By comparing Fig. 8(g), (h), (i) and (j), it can be seen that when the angle of DIP is determined, changing the angles of MIP, PIP, and MP will not affect the angle of DIP. When the angle of MIP is determined, changing the angles of PIP, MP will not affect the angle of MIP. When the angle of PIP is determined, changing the angle of MP will not affect the angle of PIP. From the above analysis, we can conclude that the four joints of the bionic finger can be driven and controlled independently to each other.

In Fig. 8, $\theta_1$ $\theta_2$ $\theta_3$ and $\theta_4$ are the rotation angles of DIP, MIP, PIP, and MP, respectively. $p_1$ $p_2$ and $p_3$ are the air pressure of the pneumatic artificial muscles that drive the DIP, MIP, and PIP joints, respectively.

The bionic finger can not only grasp by the fingertip, as shown in Fig. 9(a) and (c), the grasping of the pen and the scissor, but also can fully utilize the phalanx portion to enclose object, as shown in Fig. 9(b), the cylinder. It can be seen that the bionic finger can perform grasping or holding by different parts of its body, and has excellent gripping performance and flexibility.

Besides, the pneumatic artificial muscles adopted into the system as actuators of the flexion joints improve the compliance of the bionic finger, which is conducive to human-machine interaction, as shown in Fig. 10. The compliance of the pneumatic artificial muscles enables the bionic finger to grasp fragile objects. More specifically, on the premise of providing a strong and precise grasping, the bionic finger could also effectively avoid hurting the grasped object.

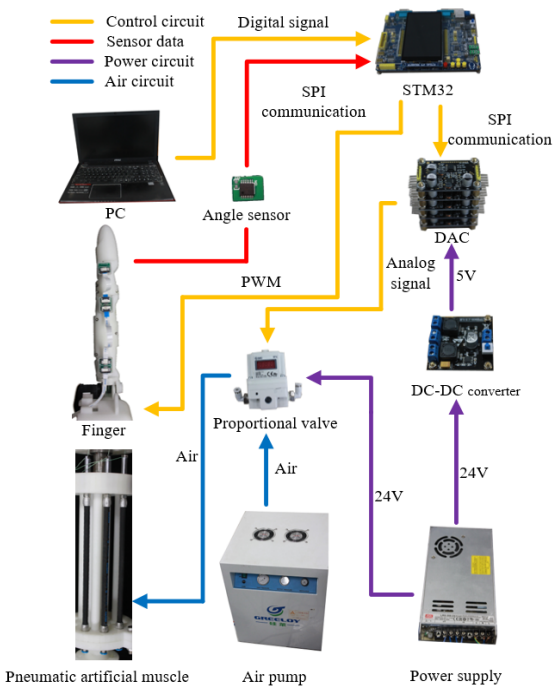


Fig. 7 Experimental platform

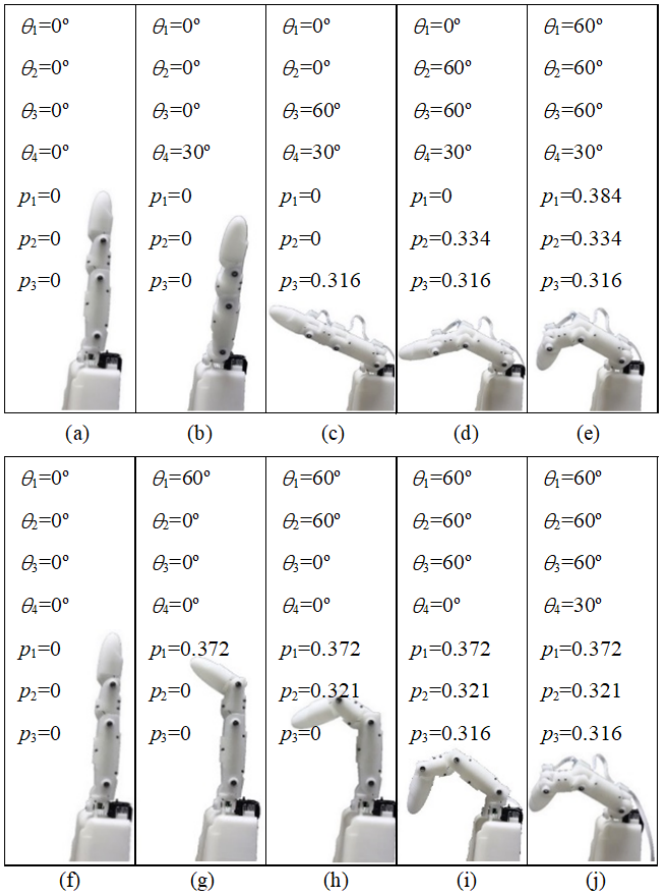


Fig. 8 Bending experiment (the units of $p_1$, $p_2$, $p_3$ are MPa)

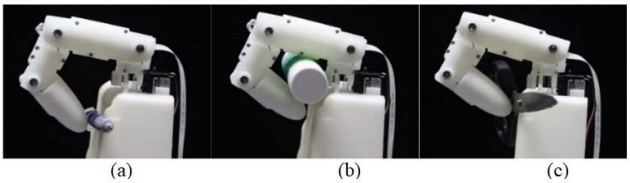

(a) (b) (c)

Fig. 9 Experiment of grasping (a) pen (b) cylinder (c) scissor

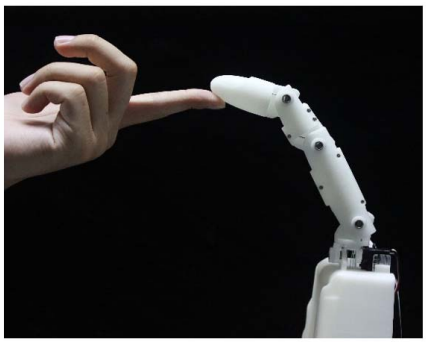

Fig. 10 Human-machine interaction

From TABLE II, it can be found that the FDB finger designed in this paper has more controllable joints but the number of actuators is the same as the DOFs.

TABLE II
TYPE OF DEXTEROUS FINGER

| Dexterous hand' finger | Number of actuators | DOFs | Number of joints |
|---|---|---|---|
| Shadow hand | 6 | 3 | 4 |
| Gifu hand III | 3 | 3 | 4 |
| Robonaut 2 Hand | 4 | 3 | 4 |
| Utah/MIT dexterous hand | 8 | 4 | 4 |
| DLR/HIT Hand II | 3 | 3 | 4 |
| FDB finger | 4 | 4 | 4 |

## IV. CONCLUSION

The article analyzes the under-actuated dexterous hand and the full-drive dexterous hand. To combine the advantages of them, we designed a full-drive decoupled bionic finger with 4 DOFs. In our design, a single tendon can independently drive each joint without causing mutual coupling. Pneumatic artificial muscles drive the three flexion joints of the finger, and a steering engine drives the swaying joint. The decoupling between the joints is achieved by the new *N* type tendon drive system and tendon route. Experiments verified the decoupling between the joints and the flexible grasping performance of the proposed finger.

## REFERENCES


[1] D. H. Lee, J. H. Park, S. W. Park, M. H. Baeg, and J. H. Bae, "KITECH-Hand: A Highly Dexterous and Modularized Robotic Hand," Ieee-Asme Transactions on Mechatronics, vol. 22, no. 2, pp. 876-887, Apr, 2017.

[2] H. Liu, et al, "Multisensory five-finger dexterous hand: The DLR/HIT hand II," 2008 IEEE/RSJ International Conference on Intelligent Robots and Systems, IROS. pp. 3692-3697.

[3] D. Alvarez, A. Lumbier, J. V. Gomez, S. Garrido, and L. Moreno, "Precision Grasp Planning with Gifu Hand III based on Fast Marching Square," 2013 Ieee/Rsj International Conference on Intelligent Robots and Systems, IEEE International Conference on Intelligent Robots and Systems N. Amato, ed., pp. 4549-4554, 2013.

[4] L. B. Zhang, Z. H. Wang, Q. H. Yang, G. J. Bao, and S. M. Qian, Development and Simulation of ZJUT Hand Based on Flexible Pneumatic Actuator FPA, 2009.

[5] C. D. Santina, C. Piazza, G. Grioli, M. G. Catalano, and A. Bicchi, "Toward Dexterous Manipulation with Augmented Adaptive Synergies: The Pisa/IIT SoftHand 2," IEEE Transactions on Robotics, vol. 34, no. 5, pp. 1141-1156, 2018.

[6] M. Controzzi, F. Clemente, D. Barone, A. Ghionzoli, and C. Cipriani, "The SSSA-MyHand: A dexterous lightweight myoelectric hand prosthesis," IEEE Transactions on Neural Systems and Rehabilitation Engineering, vol. 25, no. 5, pp. 459-468, 2017.

[7] D. Che, and W. Zhang, "A Humanoid Robot Upper Limb System with Anthropomorphic Robot Hand: GCUA Hand II," Social Robotics. pp. 182-191.

[8] L. Wang, J. DelPreto, S. Bhattacharyya, J. Weisz, and P. K. Allen, "A highly-underactuated robotic hand with force and joint angle sensors," IEEE International Conference on Intelligent Robots and Systems. pp. 1380-1385.

[9] S. A. Dalley, T. E. Wiste, H. A. Varol, M. Goldfarb, and Ieee, "A Multigrasp Hand Prosthesis for Transradial Amputees," 2010 Annual International Conference of the Ieee Engineering in Medicine and Biology Society, IEEE Engineering in Medicine and Biology Society Conference Proceedings, pp. 5062-5065, 2010.

[10] J. Sun, W. Zhang, and H. Sun, "A Novel Coupled and Self-adaptive Under-actuated Grasping Mode and the COSA-DTS Hand," Intelligent Robotics and Applications, Pt I, Lecture Notes in Artificial Intelligence H. Liu, H. Ding, Z. Xiong and X. Zhu, eds., pp. 59-70, 2010.

[11] A. Kochan, "Shadow delivers first hand," Industrial Robot, vol. 32, no. 1, pp. 15-16, 2005.

[12] L. B. Bridgwater, et al, "The Robonaut 2 Hand - Designed To Do Work With Tools," 2012 Ieee International Conference on Robotics and Automation, IEEE International Conference on Robotics and Automation ICRA, pp. 3425-3430, 2012.

[13] S. C. Jacobsen, et al, Design of the Utah/MIT dextrous hand, 1986.

[14] F. Lotti, et al, "UBH 3: an anthropomorphic hand with simplified endo-skeletal structure and soft continuous fingerpads," 2004 Ieee International Conference on Robotics and Automation, Vols 1- 5, Proceedings, Ieee International Conference on Robotics and Automation, pp. 4736-4741, 2004.

[15] H. Liu, et al, "The modular multisensory DLR-HIT-Hand: Hardware and software architecture," Ieee-Asme Transactions on Mechatronics, vol. 13, no. 4, pp. 461-469, Aug, 2008.

[16] X. H. Gao, et al, "The HIT/DLR dexterous hand: Work in progress," 2003 Ieee International Conference on Robotics and Automation, Vols 1-3, Proceedings, IEEE International Conference on Robotics and Automation ICRA, pp. 3164-3168, 2003.